JIMD Reports
DOI 10.1007/8904_2016_36

RESEARCH REPORT

White Matter Microstructure and Subcortical Gray Matter Structure Volumes in Aspartylglucosaminuria; a 5-Year Follow-up Brain MRI Study of an Adolescent with Aspartylglucosaminuria and His Healthy Twin Brother

Tokola Anna • Brandstack Nina • Hakkarainen Antti • Salli Eero • Åberg Laura • Autti Taina

Received: 6 September 2016 / Revised: 6 December 2016 / Accepted: 9 December 2016

Abstract *Objective*: Aspartylglucosaminuria is an inherited, lysosomal storage disease causing progressive decline in cognitive and motor functions. The aim of this study was to evaluate volumes of subcortical gray matter structures and white matter microstructure in aspartylglucosaminuria in adolescence in a longitudinal study for the first time.

Methods: A boy with aspartylglucosaminuria and his healthy twin brother were imaged twice with a 3.0 T MRI scanner at the ages of 10 and 15 years. Subcortical gray matter structure volumes were measured using an atlas-based automatic method, and diffusion tensor imaging was used to evaluate the white matter microstructure of the corpus callosum and the thalamocortical pulvinar tracts.

Results: The subcortical gray matter structures were smaller at onset and diminished at follow-up in the affected twin, with the exception of the amygdala which was larger and remained the size. The largest difference in volume between the twins was found in the thalami. The total gray and white matter volumes decreased in the affected twin. In diffusion tensor imaging analysis, the fractional anisotropy was decreased at onset in the affected twin compared to the healthy brother in the evaluated tracts. The axial, radial and mean diffusivity values were increased in the affected twin. The difference between the twins increased slightly at follow-up.

Interpretation: The findings suggest that volumetric measurements and diffusion tensor imaging based microstructural analysis may be useful modalities for monitoring disease progression and response to emerging treatment in aspartylglucosaminuria, but further studies with more subjects are necessary to confirm the results.

Communicated by: Nicole Wolf, M.D., Ph.D.

The original version of this chapter was revised: The Acknowledgement and Funding information was included. The erratum to this chapter is available at DOI 10.1007/8904_2017_18

Electronic supplementary material: The online version of this chapter (doi:10.1007/8904_2016_36) contains supplementary material, which is available to authorized users.

T. Anna (✉) · B. Nina · H. Antti · S. Eero · A. Taina
HUS Medical Imaging Center, Radiology, University of Helsinki and Helsinki University Hospital, Helsinki, Finland
e-mail: anna.tokola@hus.fi

Å. Laura
Department of Psychiatry, University of Helsinki and Helsinki University Hospital, Helsinki, Finland

Introduction

Aspartylglucosaminuria (AGU) is an inherited, autosomal recessive, progressive neurodegenerative disease. It belongs to lysosomal storage disorders and manifests with progressive decline in cognitive and motor functions, leading to premature death (Autti et al. 1997). Clumsiness and delayed speech development are usually the first symptoms noted in early childhood. Despite the ongoing disease, children learn new skills up until their teenage years, though more slowly than healthy children. Thereafter, learned skills are gradually lost, resulting in severe intellectual disability and deterioration of motor skills (Arvio and Arvio 2002).

The disease is caused by a mutation of the *AGA* gene located on 4q34.3, resulting in deficient activity of aspartylglucosaminidase, a lysosomal hydrolase enzyme (Saarela et al. 2001). As a result, there is excessive accumulation of uncleaved glycoasparagines in lysosomes and elevated metabolite levels in urine.

There is yet no treatment available to cure or slow down the progression of AGU. Mouse model studies investigating virus-mediated gene therapy and enzyme replacement therapy in AGU have shown some promise (Dunder et al. 2000; Virta et al. 2006). Also, small molecule compounds which may be suitable for chaperone therapy of AGU have been identified in a recent study (Banning et al. 2016). At the moment, objective modalities are needed for indexing illness stage and monitoring response to emerging treatment.

Previous brain magnetic resonance imaging (MRI) studies have revealed a typical combination of findings in AGU, including decreased T2 signal intensity (SI) in the thalami and especially the pulvinar nuclei, high T2 SI in the periventricular white matter (WM), juxtacortical high T2 SI foci and poor differentiation between gray matter (GM) and WM. Also, thin corpus callosum (CC) and some degree of cerebral and/or cerebellar atrophy are found in nearly all patients with AGU (Autti et al. 2008; Tokola et al. 2015).

Modern MRI-based methods provide more detailed information about volumetric and structural changes caused by disease processes. Brain volumes including subcortical GM structure volumes may be calculated using automated or semi-automated methods (Zhang et al. 2001; Fischl et al. 2002; Jenkinson et al. 2012). Diffusion tensor imaging (DTI) allows quantification of tissue architecture through both the degree and directionality of tissue water diffusion within a voxel, and can be used to noninvasively estimate WM tract integrity in vivo (Basser and Pierpaoli 1996).

We evaluated changes in total WM, total GM and subcortical GM structure volumes, and WM microstructure in an adolescent with AGU during a 5-year follow-up to better understand the disease process and find potential tools for indexing the illness stage in AGU. Adolescence is a unique period in the human lifespan, and various morphometric changes occur in the still-developing brain. In AGU, the typical turning point in motor and cognitive development makes this phase intriguing for investigation. Based on the age phase and pathophysiology of the disease, we hypothesized that there is volume reduction of subcortical GM structures and microstructural changes in WM tracts in the affected twin already at onset, and a progression at follow-up was expected.

Materials and Methods

Study Participants

The boy with AGU was born after a full-term twin pregnancy with a cesarean section. The early motor developmental milestones were reached within normal range. He learned to walk at the age of 15 months and had his first words at the age of 18 months. At the age of 3, speech therapy was initiated because of delayed speech. As part of etiological examinations for the developmental delay, a urine sample was collected and revealed increased amounts of aspartylglucosamine. The diagnosis of aspartylglucosaminuria was confirmed at age 5.

At the time of the first examination at 10 years of age, mild problems of coordination and balance were noticed. He was prepubertal. The cognitive performance was at the level of mild mental retardation.

At the time of the second examination at the age of 15 years, problems with coordination and balance were pronounced. Furthermore, dysarthria was observed in speech. The pubertal status was G3-4, P4. In the psychological examination, the cognitive performance had decreased as compared with levels for his age, being at the level of moderate mental retardation. No epileptic seizures had occurred.

The healthy dizygotic twin brother developed normally and had normal school history. His puberty preceded the puberty of the affected twin. He had a sports injury at the age of 14 years causing a small impacted, left-sided temporal skull fracture, which was operated. No persistent intracerebral changes were caused by the injury and the artifacts from the skull fixation material were minor, not causing disruption to the subcortical GM structures or WM tracts evaluated in the study.

The twins were imaged twice with 3.0 T brain MRI during a 5-year follow-up. The first examination was performed at the age of 9.9 years and the second at the age of 15.1 years. As a twin, the control person was age, sex and environment matched and shared around 50% of the genome. Informed consent was obtained from the parents of the twins prior to the study. A clinical neurological examination was performed on the siblings and data on their medical history was collected from the parents and medical records. No sedation was used during the scanning and the brothers were in good physical condition at the time of the examinations.

The study was approved by the local ethics committee.

MRI Acquisition

The MR imaging was performed using a 3.0 T scanner (Achieva, Philips Medical Systems, Best, The Netherlands). The examination included a T2 (Turbo spin echo) TSE axial series (TR 4,000 ms, TE 80 ms, slice thickness 4 mm, flip angle 90°, matrix 512 × 512), a T1 3D Turbo field echo (TFE) series with isotropic voxel size (TR 8.3, TE 3.8, flip angle 8°, matrix 256 × 256) and a diffusion tensor series (single-shot diffusion weighted sequence, TR 10,600 ms, TE 59.5 ms, 16 diffusion gradients, 32 + 1 directions, NA 2, matrix 112 × 112, FOV 224 × 224, $b = 1{,}000$ s/mm^2, 1 $b = 0$).

Visual Analysis

Visual analysis of the T1 and T2 weighted images was performed by two radiologists. The first examination of the affected twin had been included in a previous study (Tokola et al. 2015).

MR Image Segmentation

MR image segmentation was carried out by two different and complementary processing pipelines. In the first, we segmented the brain into tissue classes (GM, WM and CSF). In the second pipeline, we assigned neuroanatomical labels to subcortical GM structures (segmentation of anatomical classes).

The segmentation of tissue classes was performed by FMRIB Software Library v5.0 (FSL) (Jenkinson et al. 2012). First, the Brain Extraction tool (BET) was used to delete non-brain tissue from the MR images. The result was manually corrected where necessary. Then, FMRIB's Automated Segmentation Tool (FAST) was used to segment the brain-extracted images into GM, WM and CSF using the default options. The volumes of GM, WM and CSF were estimated using the partial volume estimates (Zhang et al. 2001).

The segmentation of subcortical GM structures (left and right thalami, hippocampi, amygdala, nucleus caudatus, putamen, globus pallidus and accumbens) was carried out by using the volume-based (subcortical) stream of the FreeSurfer image analysis suite (Fischl et al. 2002). The total volumes of the structures (left + right) are presented in Table 1. This method is based on both subject-specific measured values and on the alignment with a subject-independent probabilistic atlas (MNI305).

The segmentations of subcortical structures were visually checked for errors by two radiologists and minor manual corrections were made using Slicer 4 (Fedorov et al. 2012) and the nac-hncma-atlas (Halle et al. 2015). The consensus of opinion was used for the volumetric measurements.

Tractography

DTI data was processed and analysed using tools in FMRIB Software Library v5.0 (Jenkinson et al. 2012). Eddy current distortions and minor head motions were corrected using eddy correction following brain extraction from the skull and creating brain masks using bet2. Diffusion tensors, fractional anisotropy (FA), mean diffusivity (MD) and axial diffusivity (AD = $\lambda 1$) were determined using dtifit and radial diffusivity (RD) was calculated with fslmaths as $(\lambda 2 + \lambda 3)/2$. A distribution of diffusion parameters was built for each voxel on the basis of Markov Chain Monte Carlo (MCMC) by bedpostx. Two fibers per voxel were modelled and 1,000 iterations before sampling was used. Probabilistic tractography analysis of the CC frontal projections and the thalamocortical tracts from the pulvinar nuclei were carried out with probtrackx2 (5,000 sample pathways, curvature threshold 0.4, step length 0.5 mm and subsidiary fiber volume fraction threshold 0.01) utilising seed, exclusion and inclusion masks as described in detail in Supplementary Fig. 1. The masks were delineated by two radiologists and the mean values are presented. The protocol for CC frontal projections was modified from Huang et al. (2005), and the pulvinar masks were delineated based on the nac-hncma-atlas (Halle et al. 2015). Tract volumes were thresholded at 0.5% and used as masks to assess mean FA, MD, AD and RD along the tract.

Results

MRI Findings

At the age of 10 years, typical findings associated with AGU were noticed in visual evaluation. In T2-weighted images, an SI decrease in the thalami, more intense SI decrease in the pulvinar nuclei and mild periventricular SI increase were found in the images of the affected twin. Also, poor differentiation between GM and WM, mild lateral ventricle dilatation, thin corpus callosum, pineal multilocular cyst (6 mm) and some prominent perivascular spaces were seen. The skull thickness in the occipital bone of the affected twin was 6 mm, which was twice as much as the skull of the unaffected twin. No patchy WM lesions were noted. The cerebral and cerebellar atrophy was evaluated as mild.

At the age of 15 years, there was no change in the thalamic or periventricular SI alterations, but differentiation between GM and WM was better, especially in the frontal lobe. A slight progression of cerebral and cerebellar atrophy was noted.

No pathological changes were found in the visual evaluation of the images of the unaffected twin, except for small areas of artifact in the follow-up images caused by cranial fixation implants in the left temporal region.

The main findings on T1- and T2-weighted images are shown in Fig. 1.

Volumetry

The delineation of the subcortical GM structures is presented in Fig. 2 and the change in volumes at follow-up in Fig. 3. The volumes and the percentage change are also presented in Table 1.

Table 1 Brain volumes and subcortical gray matter volumes of an adolescent boy with aspartylglucosaminuria and his healthy twin brother

	Age (years)	TBV	GM	WM	CSF	Thalami	Hippocampi	Amygdala	Caudatus	Putamen	Pallidum
Patient	9.9	1,314.21	790.28	523.93	239.61	12.82	10.11	3.93	8.07	10.76	3.50
	15.1	1,251.28	737.07	514.21	297.67	12.00	9.63	3.92	7.86	9.80	3.25
Change[a]		−4.8%	−6.7%	−1.9%	24.2%	−6.4%	−4.7%	−0.3%	−2.6%	−8.9%	−7.1%
Control	9.9	1,307.06	739.94	567.12	250.42	18.01	9.88	3.34	8.33	10.99	3.51
	15.1	1,308.15	725.81	582.34	284.38	17.95	10.18	3.74	8.95	10.86	3.48
Change[a]		0.1%	−1.9%	2.7%	13.6%	−0.3%	3.0%	11.7%	7.4%	−1.2%	−0.9%
Difference patient vs. control[b]	9.9	0.5%	6.8%	−7.6%	−3.8%	−28.8%	2.3%	17.7%	−3.1%	−2.1%	−0.3%
	15.1	−4.4%	1.6%	−11.7%	4.7%	−33.1%	−5.4%	5.1%	−12.2%	−9.8%	−6.6%

The volumes are all shown in cm^3 and the subcortical volumes are sums of the left and right volume

[a] The change during follow-up is presented as percentage change from original volume

[b] Difference between the volumes of the patient and healthy twin are presented as percentage comparing the volume of the patient with the volume of healthy twin. *TBV* total brain volume, *GM* total gray matter, *WM* total white matter

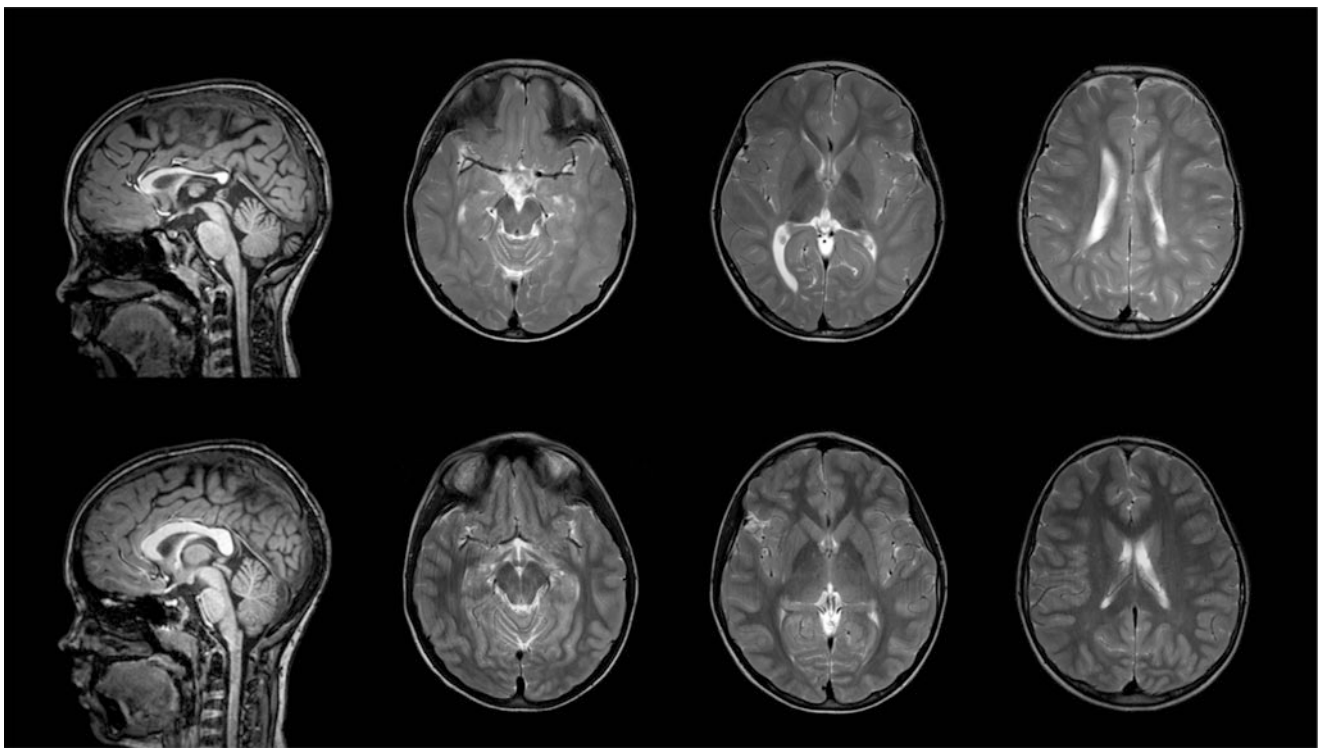

Fig. 1 Typical changes in aspartylglucosaminuria, 3.0 T T1-weighted sagittal and T2-weighted axial images. *Top row*, male patient at the age of 10 years, showing decreased signal intensity in the pulvinar nuclei of the thalami bilaterally, and signs of delayed myelination and increased signal intensity in the deep white matter in the T2-weighted images. Thin corpus callosum, mild ventricular dilatation and some slightly prominent sulci are also visible. *Second row*, healthy twin brother imaged at the same age with normal findings

At 10 years of age, the estimated total brain volume (TBV) was nearly equal between the twins, being 0.5% larger in the affected twin. At follow-up, TBV of the twin with AGU decreased by 5% and at 15 years of age, it was 4% less than the TBV of the unaffected twin. The total volume of GM was larger in the affected twin than his healthy twin brother at both time points. At onset, the total GM volume was 7% larger in the affected twin. At

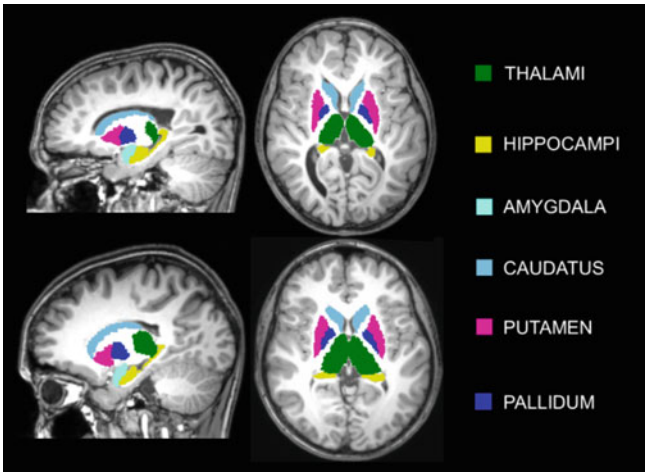

Fig. 2 Segmentation of the subcortical gray matter structures using an atlas-based method by Freesurfer. The color-coded structures are superimposed on T1-weighted images. *Top row*, patient at the age of 15 years and *second row*, healthy twin brother at the same age

follow-up, the total GM volume decreased substantially in the affected twin, by 7%, but it was still 2% larger compared with the healthy twin.

At 10 years of age, most of the subcortical GM structures were smaller in the twin with AGU than his healthy brother. The largest difference in volume was found in the thalami, which were 29% smaller at onset. The only structures that were substantially larger in the affected than the unaffected twin were amygdala, which were 18% larger. The amygdala was also the only structure to remain the size in the affected twin. Other subcortical GM structures diminished 3–9% at follow-up. The largest difference in volume at 15 years of age was found in the thalami, which were 33% smaller in the twin with AGU. Automatic segmentation for accumbens did not succeed, and in our opinion, manual correction would not have been reliable. Therefore, accumbens volumes are not included.

The total WM volume was smaller already at onset in the twin with AGU, 8% less than the healthy twin's. At follow-up, the volume reduction of the WM was milder than the reduction of GM. At the age of 15 years, the total WM volume of the affected twin was 12% less than the volume of the unaffected twin. The CSF volume increased significantly by 24% in the affected twin and 13% in the healthy twin.

DTI

Results of the quantitative DTI analysis of the CC frontal projections and thalamocortical tracts from the PU are presented in Supplementary Tables 1 and 2. The DTI color map is shown in Fig. 4 and the change in DTI parameters in Fig. 5. The masks used for the tractography are shown in Supplementary Fig. 1.

The FA values were distinctly decreased in the affected twin in all tracts evaluated already at onset, and there was no remarkable change in the FA values at the 5-year follow-up.

The MD values in the tracts under evaluation were increased in the affected twin compared with the healthy twin already at onset, and the difference between the twins grew at follow-up. Also, both AD and RD values were increased in the affected twin at onset in all tracts under evaluation, the RD values more apparently. The difference between the twins in AD and RD also grew slightly at follow-up, but overall the changes in MD, RD and AD values were modest at follow-up in both twins.

The tract volumes differed substantially between the first and second examination in both twins, but there was a tendency of volume increase in the healthy twin and volume decrease in the affected twin.

Discussion

This longitudinal study revealed volume reduction in total WM, total GM and most subcortical GM structures of an adolescent AGU patient compared with the age, sex and environment matched healthy twin brother. Also, DTI with quantitative tractography detected differences in WM microstructure, and a slight progression at follow-up was noticed.

Only a few neurohistopathologic reports describing changes in AGU patients have been published. These are based on autopsy tissues of older individuals with a progressed disease. Vacuolized neurons, glial cells and endothelial cells have been found in various brain regions including cerebral cortex, cerebellum, thalami, basal ganglia and amygdala (Haltia 1975; Autti et al. 1997; Jalanko

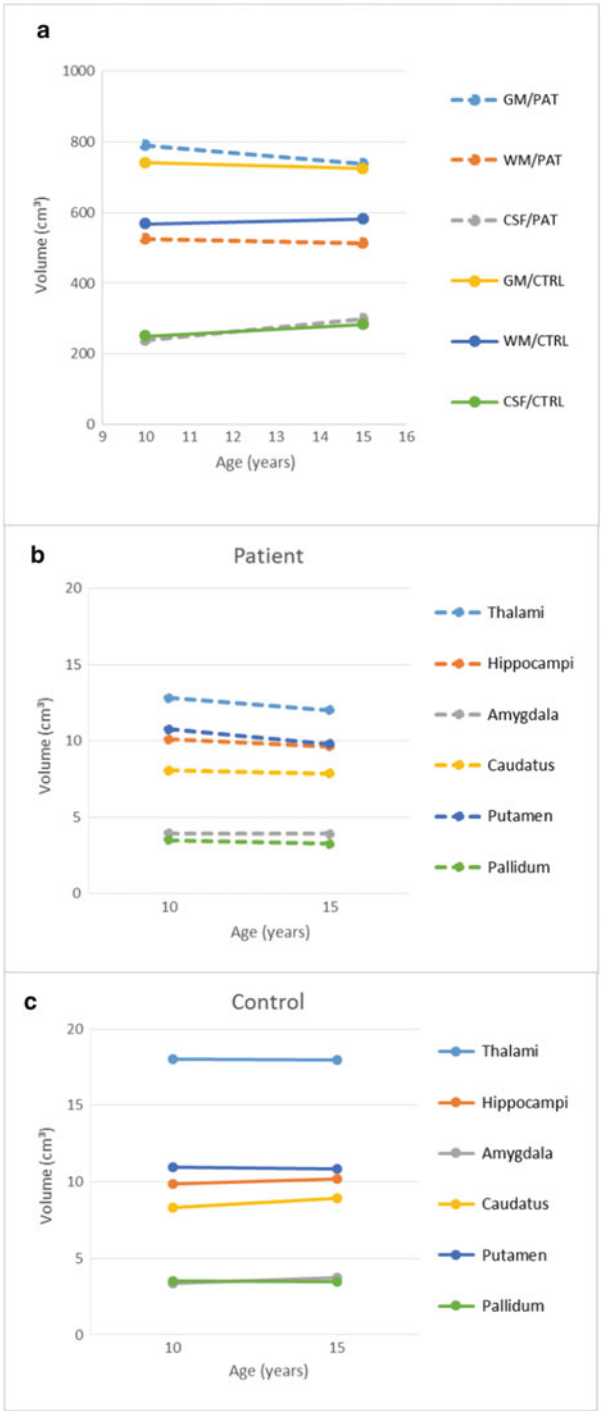

Fig. 3 (**a**) The gray matter, white matter and cerebrospinal fluid volumes of both twins at the ages of 10 and 15. The twin with AGU shows smaller white matter volume at onset but a larger gray matter volume compared with the healthy twin. The gray matter volume shows a steeper decline at follow-up. The *dotted line* represents the twin with AGU (PAT = twin with AGU, CTRL = healthy twin). (**b**, **c**) The subcortical gray matter structure volumes (*left* + *right*) of both twins at the ages of 10 and 15. The biggest difference between the brothers is seen in the thalami. In the twin with AGU, the amygdala is the only structure that does not show volume decline

et al. 1998). The basic cortical cytoarchitecture seems to be generally preserved but most neurons contain vacuoles, and the WM shows diffuse pallor of myelin staining and in some cases gliosis (Autti et al. 1997). MRI studies with volumetric evaluations and DTI based methods can provide valuable information in vivo about the changes in the brains of younger individuals with AGU.

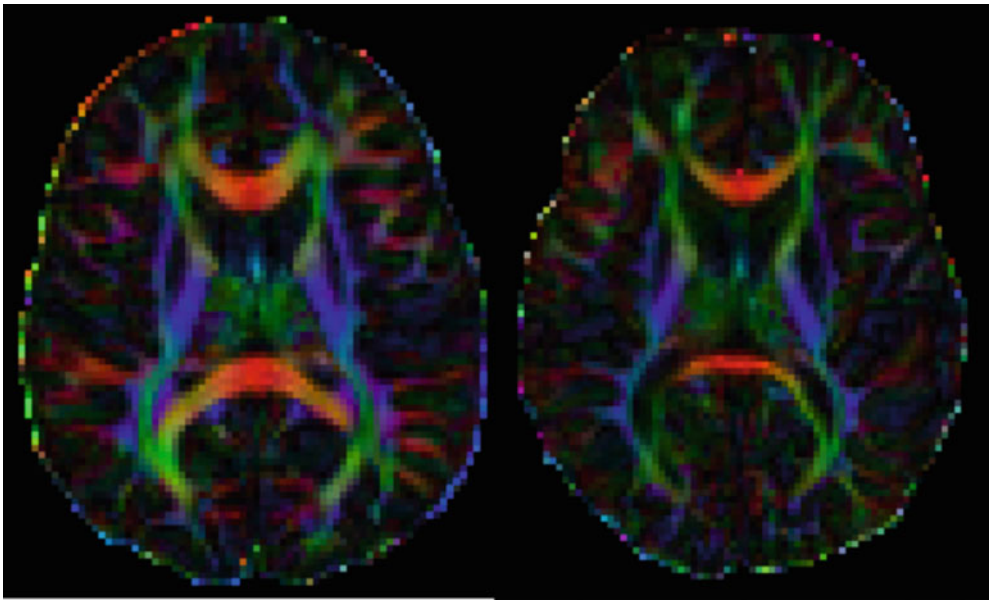

Fig. 4 DTI color map, axial images at the level of the genu of the corpus callosum overlaid on T1-weighted images. On the *left*, healthy twin at the age of 10 years and on the *right*, the twin with AGU at the same age. The figure shows color-coded white matter tracts in the transverse (*red*), longitudinal (*green*) and horizontal (*blue*) directions. There is a visible difference between the twins, with several white matter tracts being thinner in the images of the twin with AGU. Remarkable differences are noted e.g. in the genu, splenium, forceps minor and forceps major of corpus callosum

Knock-out mouse models for AGU have shown similar histopathologic findings in the CNS, including vacuolation of neurons and glial cells and signs of delayed or deficient myelination (Tenhunen et al. 1998; Jalanko et al. 1998; Gonzalez-Gomez et al. 1998). No major differences in the distribution of myelin have been detected. Vacuolation is seen also in the oligodendroglia, which may have an impact on the myelination process. Also, pathologic, hypertrophic axons have been detected in the brains of AGA−/− mice (Tenhunen et al. 1998).

Volumetry

Human brain MRI studies on healthy individuals have shown that total brain volume, GM and WM volume are highly hereditable (Thompson et al. 2002; Giedd et al. 2007). Smaller structures, perhaps because of greater proportion of measurement error, tend to have lower hereditability values and WM volumes tend to be more hereditable than GM volumes. Lower GM hereditability is consistent with the finding that plastic synapses change in response to environment and activity (Giedd et al. 2007). Some small differences in volumes in our study might be explained by normal variation between twins. Still, the most significant finding is that the difference increases between the affected twin and his healthy brother in adolescence in most volumes measured (Fig. 3).

Data from previous studies among healthy individuals indicate that the change in GM volume during adolescence has an “inverted U”-shape pattern and greater regional variation than WM (Giedd 2004; Gogtay et al. 2004; Sowell et al. 2004). Therefore, at this age in normally developing males, a slight reduction in GM volume is seen. Interestingly, in our study the total GM volume was larger in the affected twin at onset. At follow-up, the total GM volume of the affected twin decreased more than the volume of the unaffected twin, but still remained larger (Table 1). This may be explained by abnormal GM organization, considered an explanation for GM volume loss in puberty in normal development.

In contrast to the GM growth pattern, the WM volume increases almost linearly throughout adolescence (Giedd et al. 1999). In normal adolescent development, the increase in WM volume possibly reflects continuing myelination and increased axonal calibre within fiber bundles (Paus 2010). Our finding is in line with previous studies, since the total WM volume of the healthy twin increased slightly at follow-up. However, in the affected twin, the total WM volume slightly diminished between examinations, possibly related to the discontinuing myelination and loss of connections.

Even if the total GM volume in the affected twin was larger compared to the healthy twin, most of the subcortical GM structures were smaller already at onset and the volume reductions continued, as measured at follow-up. The

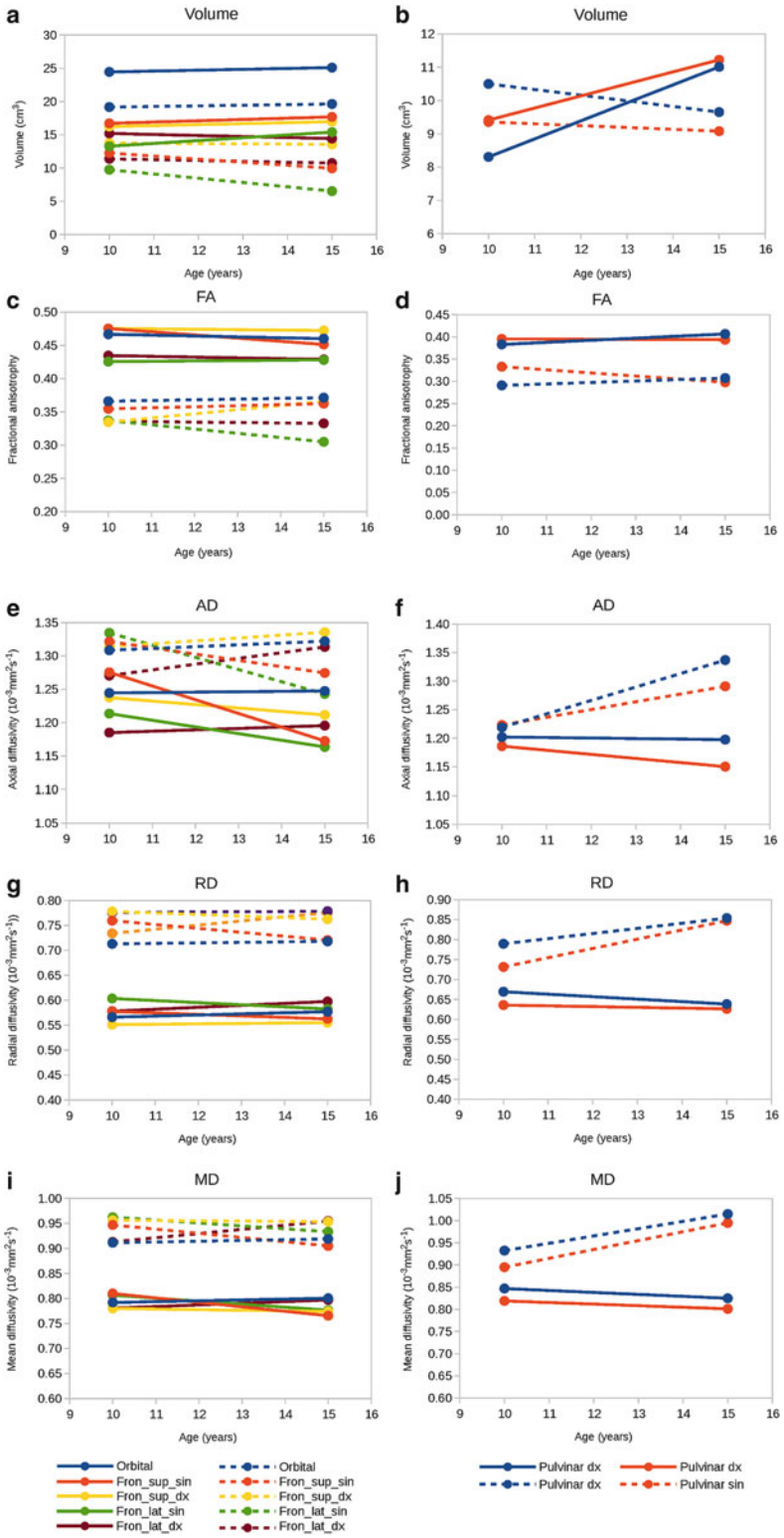

Fig. 5 Results for the quantitative diffusion tensor imaging analysis of corpus callosum frontal projections and thalamocortical pulvinar tracts. The *dotted line* represents the twin with AGU. The *left row* shows the results for the corpus callosum frontal projections and the *right row* shows the results for the thalamocortical pulvinar tracts (color coding of the tracts is explained under the diagrams). A tendency of reduction in tract volumes is seen in the affected twin (diagrams (**a**) and (**b**)). Also, decreased FA, as well as increased AD, RD and MD is noticed in the twin with AGU (diagrams (**c**)–(**j**)) in the tracts under evaluation

functions of the basal ganglia are linked to control of voluntary motor movements, but also higher cognitive function and emotions, with a major role in learning and memory. Volume reduction and dysfunction in subcortical GM structures may be involved in the progressive worsening of motor and cognitive functions that typically occurs at adolescence in AGU. The only structure to remain the same size was amygdala, which in normally developing males increases in size at this age (Wierenga et al. 2014). In the affected twin, there is probably simultaneous age-related volume increase and reduction caused by the disease.

In our study, the biggest difference in volume between the twins was found in the thalamus, in line with data suggesting that the thalamus has a central role in the pathogenesis of AGU. In previous MRI studies a decreased T2 SI in the thalami and especially pulvinar nuclei has been found even in young patients (Autti et al. 2008) and in some histopathologic studies, vacuolation has been particularly severe in the lateral nuclei of thalami and the basal nuclei (Autti et al. 1997; Gonzalez-Gomez et al. 1998). The thalamus is a paired nuclear complex serving as a relay station for sensory inputs to the cerebral cortex. It has also been suggested that the thalamus modulates information between cerebral cortical areas and is evolved in regulation of emotion, motivation and multimodal cognition. Therefore, dysfunction of the thalamus may have substantial impact on the clinical picture of AGU.

DTI

DTI allows quantification of WM integrity and organization based on the degree and directionality of tissue water diffusion. Four parameters (FA, MD, AD and RD) are used to describe WM structural properties. According to previous DTI studies on healthy individuals, the maturation of WM continues during childhood and adolescence in various areas (Barnea-Goraly et al. 2005; Lebel et al. 2008), including the areas of interest in our study. The thalamocortical pulvinar tracts and the CC frontal projections were chosen for the analysis due to previously reported MRI findings in AGU patients on conventional sequences.

We found widespread alterations to WM microstructure in the CC frontal projections and thalamocortical pulvinar tracts and the difference between the siblings was evident for all DTI parameters. As expected, the FA values were decreased in the affected twin and MD was increased, indicating microstructural disintegration and increased overall diffusion. Both the AD and RD values of the studied tracts were increased in the AGU subject. This agrees with prior findings that both the axons and the myelin are affected by the disease.

In our study, the water diffusivity was increased in the affected twin. It is possible, however, that there is simultaneous restriction (because of the vacuoles), but the increase in diffusion is emphasized. Probably the basic metabolic disturbance interferes with the growth and maturation of both neurons and glial cells, and early microstructural changes may impact the development of efficient WM fiber networks. Later, accumulation might disturb cell functions and cause cell death. Wallerian-like degeneration may also have a role in progressive general atrophy and gliosis in older individuals with AGU.

The difference in MD, AD and RD values between the siblings increased slightly at follow-up, but there was no marked age-related FA, MD, AD or RD change in our patient. This suggests that microstructural changes (including axonal membrane features and myelination level) of the CC and pulvinar tracts may occur in early childhood, and the tract volume loss in the patient is likely related to the loss of connections and GM involvement. These alterations may explain some of the motor, cognitive and emotional features of AGU.

A possible limitation of tract-based analysis is choosing the appropriate FA threshold and deflection angle (Mukherjee et al. 2008). We used a percentage threshold of 0.5% instead of a fixed threshold for the FA to reduce the effect on tract volumes. In our opinion, a fixed FA threshold could have distorted the patient results by cutting off areas of lower anisotropy.

This is a preliminary study with only one patient, which is obviously the major limitation of the study. However, FA measurements in the large Human Connectome Project are highly hereditable in major WM tracts (Kochunov et al. 2015). Also, in a prior DTI study on twins, it was noted that WM hereditability is markedly high in adolescent males (Chiang et al. 2011), which makes the twin brother in our study an especially suitable control person. Two radiologists delineated the ROIs for inclusion and exclusion masks independently to reduce subjectivity.

All examinations were performed with the same device and the same imaging protocol, minimizing variations due to technical reasons.

Future Directions

In studies of several other lysosomal storage disorders (i.e. Krabbe disease, Cystinosis, Niemann-Pick type C, Gaucher type I and II, Mucolipidosis type IV and Fabry disease), it has been suggested that GM volumetric analysis and/or quantitative DTI may be useful modalities for indexing illness stage and monitoring response to emerging treatment (Escolar et al. 2009; Bava et al. 2010; Walterfang et al. 2010; Davies et al. 2011; Schiffmann et al. 2014; Paavilainen et al. 2013). Based on our preliminary study,

automated volumetric brain analysis and quantitative DTI may be suitable biomarkers for evaluating effects of possible AGU treatments, although further studies with a larger population size, including patients from different age groups, are necessary. Moreover, complementary studies including other parts of the brain are needed to better understand the microstructural and volume changes related to AGU.

Acknowledgements The authors wish to thank the twins and their family for participating in the study and PhD Jaana Hiltunen for her assistance.

Funding This study was supported by Finnish Brain Foundation, Arvo and Lea Ylppö Foundation, Yrjö Jahnsson Foundation and Helsinki University Hospital Research Funds, Department of Radiology. No financial or other relationships that might lead to perceived conflict of interest exist.

Author Contributions

Conception and design of the study (TA, AT, NB, AH, ES), acquisition and analysis of data (AT, AH, NB, ES, LÅ), drafting the manuscript or figures (AT, NB, ES, AH, LÅ).

References

Arvio P, Arvio M (2002) Progressive nature of aspartylglucosaminuria. Acta Paediatr 91:255–257

Autti T, Raininko R, Haltia M et al (1997) Aspartylglucosaminuria: radiologic course of the disease with histopathologic correlation. J Child Neurol 12:369–375

Autti T, Lonnqvist T, Joensuu R (2008) Bilateral pulvinar signal intensity decrease on T2-weighted images in patients with aspartylglucosaminuria. Acta Radiol 49:687–692

Banning A, Gulec C, Rouvinen J et al (2016) Identification of small molecule compounds for farmacological chaperone therapy of aspartylglucosaminuria. Nat Sci Rep 6:37583

Barnea-Goraly N, Menon V, Eckert M et al (2005) White matter development during childhood and adolescence: a cross-sectional diffusion tensor imaging study. Cereb Cortex 15:1848–1854

Basser PJ, Pierpaoli C (1996) Microstructural and physiological features of tissues elucidated by quantitative-diffusion-tensor MRI. J Magn Reson B 111:209–219

Bava S, Theilmann RJ, Sach M et al (2010) Developmental changes in cerebral white matter microstructure in a disorder of lysosomal storage. Cortex 46:206–216

Chiang MC, McMahon KL, de Zubicaray GI et al (2011) Genetics of white matter development: a DTI study of 705 twins and their siblings aged 12 to 29. Neuroimage 54:2308–2317

Davies EH, Seunarine KK, Banks T, Clark CA, Vellodi A (2011) Brain white matter abnormalities in paediatric Gaucher type I and type III using diffusion tensor imaging. J Inherit Metab Dis 34:549–553

Dunder U, Kaartinen V, Valtonen P et al (2000) Enzyme replacement therapy in a mouse model of aspartylglycosaminuria. FASEB J 14:361–367

Escolar ML, Poe MD, Smith JK et al (2009) Diffusion tensor imaging detects abnormalities in the corticospinal tracts of neonates with infantile Krabbe disease. AJNR Am J Neuroradiol 30:1017–1021

Fedorov A, Beichel R, Kalpathy-Cramer J et al (2012) 3D slicer as an image computing platform for the quantitative imaging network. Magn Reson Imaging 30:1323–1341

Fischl B, Salat DH, Busa E et al (2002) Whole brain segmentation: automated labeling of neuroanatomical structures in the human brain. Neuron 33:341–355

Giedd JN (2004) Structural magnetic resonance imaging of the adolescent brain. Ann N Y Acad Sci 1021:77–85

Giedd JN, Blumenthal J, Jeffries NO et al (1999) Brain development during childhood and adolescence: a longitudinal MRI study. Nat Neurosci 2:861–863

Giedd JN, Schmitt JE, Neale MC (2007) Structural brain magnetic resonance imaging of pediatric twins. Hum Brain Mapp 28:474–481

Gogtay N, Giedd JN, Lusk L et al (2004) Dynamic mapping of human cortical development during childhood through early adulthood. Proc Natl Acad Sci U S A 101:8174–8179

Gonzalez-Gomez I, Mononen I, Heisterkamp N et al (1998) Progressive neurodegeneration in aspartylglycosaminuria mice. Am J Pathol 153:1293–1300

Halle M, Talos I, Jakab M et al (2015) Multi-modality MRI-based atlas of the brain. SPL, Boston

Haltia M, Palo J, Autio S (1975) Aspartylclucosaminuria: a generalized storage disease. Morphological and histochemical studies. Acta Neuropathol 31:243–255

Huang H, Zhang J, Jiang H et al (2005) DTI tractography based parcellation of white matter: application to the mid-sagittal morphology of corpus callosum. Neuroimage 26:195–205

Jalanko A, Tenhunen K, McKinney C et al (1998) Mice with an aspartylglucosaminuria mutation similar to humans replicate the pathophysiology in patients. Hum Mol Genet 7:265–272

Jenkinson M, Beckmann CF, Behrens TEJ, Woolrich MW, Smith SM (2012) FSL. Neuroimage 62:782–790

Kochunov P, Jahanshad N, Marcus D et al (2015) Heritability of fractional anisotropy in human white matter: a comparison of human connectome project and ENIGMA-DTI data. Neuroimage 111:300–311

Lebel C, Walker L, Leemans A, Phillips L, Beaulieu C (2008) Microstructural maturation of the human brain from childhood to adulthood. Neuroimage 40:1044–1055

Mukherjee P, Chung SW, Berman JI, Hess CP, Henry RG (2008) Diffusion tensor MR imaging and fiber tractography: technical considerations. AJNR Am J Neuroradiol 29:843–852

Paavilainen T, Lepomaki V, Saunavaara J et al (2013) Diffusion tensor imaging and brain volumetry in Fabry disease patients. Neuroradiology 55:551–558

Paus T (2010) Growth of white matter in the adolescent brain: myelin or axon? Brain Cogn 72:26–35

Saarela J, Laine M, Oinonen C et al (2001) Molecular pathogenesis of a disease: structural consequences of aspartylglucosaminuria mutations. Hum Mol Genet 10:983–995

Schiffmann R, Mayfield J, Swift C, Nestrasil I (2014) Quantitative neuroimaging in mucolipidosis type IV. Mol Genet Metab 111:147–151

Sowell ER, Thompson PM, Toga AW (2004) Mapping changes in the human cortex throughout the span of life. Neuroscientist 10:372–392

Tenhunen K, Uusitalo A, Autti T et al (1998) Monitoring the CNS pathology in aspartylglucosaminuria mice. J Neuropathol Exp Neurol 57:1154–1163

Thompson P, Cannon TD, Toga AW (2002) Mapping genetic influences on human brain structure. Ann Med 34:523–536

Tokola AM, Aberg LE, Autti TH (2015) Brain MRI findings in aspartylglucosaminuria. J Neuroradiol 42:345–357

Virta S, Rapola J, Jalanko A, Laine M (2006) Use of nonviral promoters in adenovirus-mediated gene therapy: reduction of lysosomal storage in the aspartylglucosaminuria mouse. J Gene Med 8:699–706

Walterfang M, Fahey M, Desmond P et al (2010) White and gray matter alterations in adults with Niemann-pick disease type C: a cross-sectional study. Neurology 75:49–56

Wierenga L, Langen M, Ambrosino S, van Dijk S, Oranje B, Durston S (2014) Typical development of basal ganglia, hippocampus, amygdala and cerebellum from age 7 to 24. Neuroimage 96:67–72

Zhang Y, Brady M, Smith S (2001) Segmentation of brain MR images through a hidden Markov random field model and the expectation-maximization algorithm. IEEE Trans Med Imaging 20:45–57